Research article

Xu Dong Gao, Guang Tao Fei*, Shao Hui Xu, Bin Nian Zhong, Hao Miao Ouyang, Xin Hua Li and Li De Zhang

# Porous Ag/$TiO_2$-Schottky-diode based plasmonic hot-electron photodetector with high detectivity and fast response

https://doi.org/10.1515/nanoph-2019-0094
Received March 27, 2019; revised May 13, 2019; accepted May 15, 2019

**Abstract:** Due to the advantages of narrow energy distribution of plasmonic hot-electrons in Ag and the high density of states in the $TiO_2$ conduction band, an Ag/$TiO_2$ composite is considered to be an ideal combination to construct a plasmonic hot-electron photodetector with high detectivity and a high response speed. In this work, we fabricate a porous Ag/$TiO_2$-Schottky-diode based plasmonic hot-electron photodetector. This detector shows a high detectivity of $9.8\times10^{10}$ cmHz$^{1/2}$/W and a fast response speed, with a rise and fall time of 112 μs and 24 μs, respectively, under 450 nm light illumination at zero bias voltage. In addition, the height of the Ag/$TiO_2$ Schottky barrier can be decreased by removing the chemisorbed oxygen from the surface of $TiO_2$ with ultraviolet light illumination, and as a result, the responsivity of the Ag/$TiO_2$ plasmonic hot-electron photodetector at 450 nm can increase from 3.4 mA/W to 7.4 mA/W.

**Keywords:** photodetector; plasmonic hot-electron; porous Ag/$TiO_2$; Schottky junction.

## 1 Introduction

Plasmonic hot-electrons are highly energetic electrons that are generated in metal in the decay of surface plasmons [1]. The combination of an appropriate plasmonic metal and semiconductor to form a metal/semiconductor Schottky junction can transform light energy to other forms of energy via the plasmonic hot-electrons, and they have a wide application in photocatalysis [2], photoelectrochemical water splitting [3], photovoltaic conversion [4], photodetection [5–7] and so on. The plasmonic hot-electron photodetector composed of a metal/semiconductor Schottky junction is a new kind of photodetector [8–11] which has the advantages of enabling a response to the photons with energy below the bandgap of the semiconductor substrate and having a tunable spectral response peak by simply adjusting the metal nanostructure [7, 12], therefore attracting a great deal of attention. In the past several years, much effort has been focused on improving the performance of photovoltaic hot-electron photodetectors. With the evolution of the plasmonic metal materials from separated nanorods to integrated nanoporous membranes, the responsivity of the Au/Si photovoltaic hot-electron photodetectors has increased from 8 nA/mW to 8.2 μA/mW in the near-infrared region [7, 13–15]. However, the detectivity and response time of a photovoltaic hot-electron photodetector, which are of more importance than the responsivity in the applications of optical imaging and optical communication [16], have not improved much.

An Ag/$TiO_2$ Schottky junction is considered to be an ideal material for a plasmonic hot-electron photodetector. On the one hand, although most of the plasmonic hot-electron photodetectors developed recently are based on Au/semiconductor-Schottky-diodes [7, 13–15, 17–20], Ag is considered to be a better plasmonic material than Au due to the higher density of plasmon electric fields [21] and narrower energy distribution of generated hot-electrons in Ag [1], and as a result, it can lead to a higher photoelectric conversion efficiency. On the other hand, $TiO_2$ is by far the most frequently used electron-accepting material and the high density of states in the $TiO_2$ conduction band enables fast electron injection [22, 23]. Thus, the hot-electron photodetector based on a Ag/$TiO_2$ Schottky junction may have high detectivity and a fast response speed. However, the

***Corresponding author: Guang Tao Fei,** Key Laboratory of Materials Physics and Anhui Key Laboratory of Nanomaterials and Nanotechnology, Institute of Solid State Physics, Hefei Institutes of Physical Sciences, Chinese Academy of Sciences, Hefei, Anhui 230031, P.R. China, e-mail: gtfei@issp.ac.cn. https://orcid.org/0000-0002-4657-1285
**Xu Dong Gao, Shao Hui Xu, Bin Nian Zhong, Hao Miao Ouyang, Xin Hua Li and Li De Zhang:** Key Laboratory of Materials Physics and Anhui Key Laboratory of Nanomaterials and Nanotechnology, Institute of Solid State Physics, Hefei Institutes of Physical Sciences, Chinese Academy of Sciences, Hefei, Anhui 230031, P.R. China

fabrication of a Ag/$TiO_2$ Schottky junction is full of challenges due to the fact that the work function of Ag is too low for Ag to form a Schottky contact with n-type $TiO_2$ [24], so that the Ag/$TiO_2$ based hot-electron photodetector has not yet been developed successfully. Recently, our work showed that the chemisorbed oxygen on the surface of $TiO_2$ can change the surface energy band of $TiO_2$, which enables the formation of Schottky contact between $TiO_2$ and Ag [24].

In this work, we synthesized a porous Ag/$TiO_2$-Schottky-diode based plasmonic hot-electron photodetector, and systematically studied its performance. This photodetector shows a fast response speed with a rise and fall time of 112 μs and 24 μs, respectively, and a high detectivity of $9.8\times10^{10}$ cmHz$^{1/2}$/W under 450 nm light illumination at zero bias voltage; both of these values are substantially better than those previously reported. By decreasing the Schottky barrier through a long-hours ultraviolet light illumination process, the responsivity of the device at 450 nm increased from 3.4 mA/W to 7.4 mA/W.

# 2 Experiments

## 2.1 Device fabrication

The $TiO_2$ nanoporous membrane was fabricated by electrochemical anodization of Ti foil (Tianmai Titanium Industry Ltd., Baoji, Shaanxi, China) in electrolyte [25]. Before anodization, the Ti foil was degreased by sonication in acetone (Sinopsin Group Chemical Reagent Ltd., Shanghai, China) and ethanol (Sinopsin Group Chemical Reagent Ltd., Shanghai, China) sequentially, and then dried in air. Afterwards, pre-anodization of the Ti foil was carried out in ethylene glycol solutions containing 0.3 wt% $NH_4F$ and 2 vol% $H_2O$ at a constant voltage of 60 V for 2 h at 20°C, and then the formed $TiO_2$ membrane on the Ti foil was removed by sonication in deionized water, leaving ordered concaves on the Ti foil. Subsequently, the Ti foil with ordered concaves on the surface was anodized again in ethylene glycol solutions containing 0.3 wt% $NH_4F$ (Sinopsin Group Chemical Reagent Ltd., Shanghai, China) and 6 vol% $H_2O$ at a constant voltage of 60 V for 1 min to obtain a thin $TiO_2$ nanoporous membrane on the Ti foil. After rinsing in ethanol, the $TiO_2$/Ti foil was annealed at 400°C in air for 3 h to obtain anatase $TiO_2$ membrane. Finally, the annealed $TiO_2$/Ti foil was covered with a mask, and then an Ag layer with thickness of about 30 nm was sputtered on it by the sputter coater (Emitech K550x) in a vacuum of 10 Pa at a current of 40 mA for 3 min. Peeling off the mask, a photodetector device with a working area of 28 mm$^2$ was obtained.

## 2.2 Device characterization

The current–voltage (I–V) curves and photocurrent response of the sample were measured by a Keithley semiconductor parameter analyser (4200-SCS, Keithley Instruments Inc., Cleveland, OH, USA) model 4200-SMU with the sample placed in a probe station (TTPX, Lake Shore Cryotronics lnc., Westerville, OH, USA) under a vacuum environment of $6\times10^{-4}$ Pa. A 500 W xenon lamp (GLORIA-X500A, Zolix Inc., Beijing, China) equipped with a monochromator (iHR320, Horiba lnc., Piscataway, NJ, USA) was used as the tunable light source for spectral photoresponse characterization, while tunable power lasers (RD450-1000F3, RD660-1000F3, and RD980-1000F3, Richeng Science & Technology Inc., Xi'an, Shaanxi, China) were used as 450 nm, 660 nm, and 980 nm light sources, respectively, and an LED light (XPE-365nm, Cree Inc., Durham, NC, USA) with a central wavelength of 365 nm was used as the light source for ultraviolet light illumination. An electronic timer (GCI-73, Daheng Science & Technology Inc., Beijing, China) was used to control the switch of the light path to generate the low-frequency (<1 Hz) pulsed light. High-frequency (>1 Hz) pulsed 450 nm light was provided by a pulsed laser (RD450-1000G3, Richeng Science & Technology Inc., Xi'an, Shaanxi, China). The time response of the device to the high-frequency pulsed light was measured by a Keithley semiconductor parameter analyser (Keithley 4200-SCS) model 4200-PMU.

The surface morphology of the sample was characterized by field-emission scanning electron microscopy (SU8020, Hitachi, Ltd., Tokyo, Japan). The crystal structure of the sample was identified by X-ray diffraction using a X-ray diffractometer (Philips X'Pert Pro MPD, PANalytical B.V., Almelo, The Netherlands) equipped with a Cu Kα1 ($\lambda = 0.15406$ nm) radiation source. The optical transmittance was measured using a UV-vis dual-beam spectrophotometer (CARY-5E, Varian Australia Pty Ltd., Mulgrave, Victoria, Australia).

# 3 Results and discussion

## 3.1 Porous Ag/$TiO_2$-Schottky-diode and plasmonic photoelectric response

The porous Ag/$TiO_2$ photodetector consists of a porous Ag layer, an anatase porous $TiO_2$ membrane (Figure S1) and a Ti substrate electrode (the inset of Figure 1A). The porous Ag layer can absorb light to generate plasmonic hot-electrons, and the porous $TiO_2$ membrane is used as

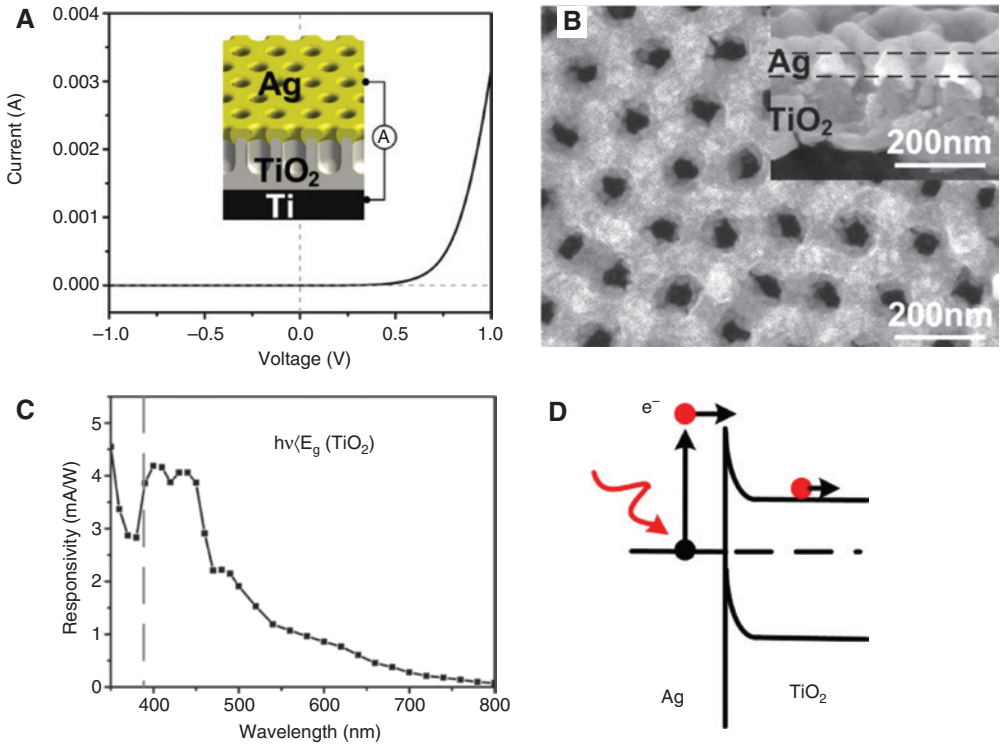


**Figure 1:** Photodetector structure and plasmonic hot-electron participated photoresponse.
(A) Schottky I–V curve of porous Ag/$TiO_2$ composite film measured in vacuum. (B) Scanning electron microscopy images of the porous Ag/$TiO_2$ membrane. (C) Spectral responses of the porous Ag/$TiO_2$ photodetector. (D) Band diagram for the generation of plasmonic hot-electrons photocurrent.

electron-accepting material. The I–V curve of the device exhibited a typical rectifying behavior, proving that the fabricated Ag/$TiO_2$ heterojunction is a Schottky junction (Figure 1A). The Schottky barrier height was calculated to be 0.83 eV (detailed calculation process refers to Supplementary note and Figure S2). Figure 1B shows scanning electron microscopy images of the porous Ag/$TiO_2$ membrane; the ordered pores showed a period of 120 nm. In addition, it is clear to see that the thickness of the Ag layer and the $TiO_2$ membrane were approximately 50 nm and 150 nm, respectively. Due to the low vacuum sputtering condition, the sputtering silver atoms have low collimation, resulting in the sputtering silver atoms mainly reaching the surface of the pores and forming a cap shape coverage.

Such a porous Ag/$TiO_2$-Schottky-diode is a self-powered plasmonic hot-electron photodetector that can work under zero voltage. The response spectrum of the photodetector ranged from visible to near-infrared with a responsivity peak of 4 mA/W at 440 nm (Figure 1C). Because the energy of the visible light (1.6–3.1 eV for 400–780 nm photons) was lower than the bandgap of anatase $TiO_2$ (3.17 eV) [24, 26, 27], the photoresponse shown in Figure 1C is believed to be a plasmon-participating photoresponse, which can be proved by the agreement in wavelength between the photocurrent responsivity peak and surface plasmon resonance peak of the porous Ag/$TiO_2$ membrane (Figure S3) [14, 24, 28]. Figure 1D illustrates the energy band diagram for the plasmon-participating photoresponse, where incident light excites surface plasmons on the porous Ag layer and some of the plasmons then decay into hot-electrons and holes [29]. The hot-electrons with enough energy will jump across the Schottky barrier at the Ag/$TiO_2$ interface and then contribute to a detectable photocurrent.

## 3.2 High detectivity and fast response

Figure 2A shows the photoresponse of the Ag/$TiO_2$ photodetector to the light with a wavelength of 450 nm at zero bias voltage, where the on-off interval of the light was 30 s. Our device clearly displayed a rapid and stable response to the pulsed light. Furthermore, the photocurrent of the device almost kept a linear relationship with the incident light power (Figure 2B).

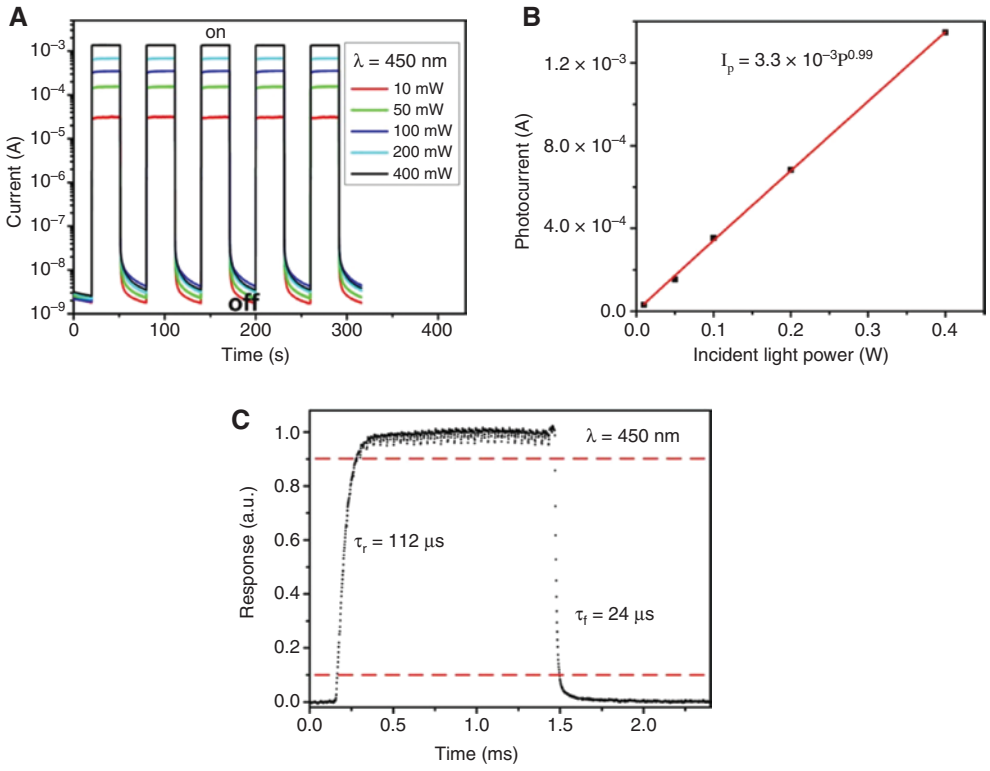


**Figure 2:** Photocurrent response under 450 nm light illumination.
(A) Response under pulsed light illumination with different power at zero bias voltage. (B) Fitting curve of the relationship between the photocurrent and light power. (C) A single normalized cycle of the photocurrent response.

To quantify the performance of the porous Ag/$TiO_2$ photodetector, three key metrics, viz., responsivity (R), external quantum efficiency (η) and detectivity (D*), were calculated by using the following equations [30]:

$$R = I_p / P \tag{1}$$

$$\eta = (I_p / e) / (P / h\nu) = (hc / \lambda e)(I_p / P) \tag{2}$$

$$D^* = S^{1/2} R / (2eI_d)^{1/2} \tag{3}$$

where $I_p$, P, h, c, λ, e, S and $I_d$ are the photocurrent, incident light power, Planck's constant, speed of light, light wavelength, unit of elementary charge, working area of the photodetector and dark current, respectively. Using the data presented in Figure 2A, we calculated the responsivity R and the external quantum efficiency η to be 3.3 mA/W and 0.91%, respectively; these values are comparable to the results reported for the Si-based hot-electron near-infrared photodetector with R of 3.5 mA/W and η of 0.35% [14]. On the basis of the S value of 28 $mm^2$ and the $I_d$ value of 1 nA, the detectivity D* was estimated to be $9.8 \times 10^{10}$ $cmHz^{1/2}/W$.

The minimum detectable light intensity ($E_{min}$) is another important metric, which is defined as the incident light intensity when the generated photocurrent ($I_p$) is equal to the dark current ($I_d$). As $R = I_p/P$ and $P = E \cdot A$, so $E = I_p/(R \cdot A)$, where $I_p$, R, P, E, and A are the photocurrent, responsivity, incident light power, incident light intensity, and working area of the photodetector, respectively. When $I_p = I_d$, $E_{min}$ can be obtained by the equation $E_{min} = I_p/(R \cdot A) = J_d/R$, where $I_d$ and $J_d$ are the dark current and dark current intensity, respectively. Owing to the current-limiting effect of the Schottky barrier at the Ag/$TiO_2$ interface, the dark current intensity ($J_d$) was only 3.6 $nA/cm^2$, which contributed to a low $E_{min}$ of only $1.1 \times 10^{-6}$ $W/cm^2$ that was more superior than other reported photovoltaic plasmonic hot-electron photodetectors [7, 15, 20].

In addition to the aforementioned metrics, the response speed is also a key parameter for practical applications of a photodetector in optical communications and optical switches, which is often evaluated by the rise time ($\tau_r$) and the fall time ($\tau_f$) of its response to a pulsed signal [16, 30, 31], where $\tau_r$ and $\tau_f$ are always defined as the time intervals required for the photocurrent to rise from 10% to 90% of its peak value ($\tau_r$) and for the response to decay from 90% to 10% of its peak value ($\tau_f$) [30]. As shown in

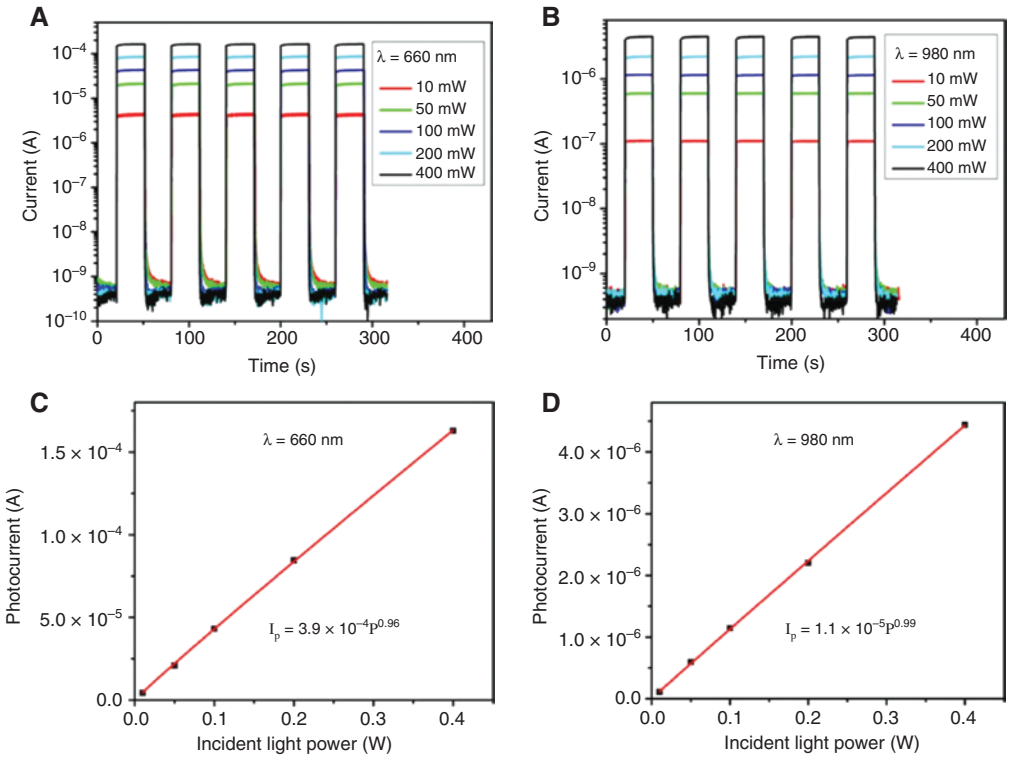


**Figure 3:** Photoresponse under 660 nm and 980 nm light illumination.
(A) Photocurrent response under 660 nm light illumination. (B) Photocurrent response under 980 nm light illumination. (C) $I_p$–P curves under 660 nm light illumination. (D) $I_p$–P curves under 980 nm light illumination.

**Table 1:** Comparison of the device performance of the present porous Ag/$TiO_2$ photodetector with other plasmonic hot-electron photodetectors.

| Device | R (A/W) | D* (cmHz$^{1/2}$/W) | $\tau_r/\tau_f$ | $E_{min}$ (W/cm$^2$) | Ref. |
|---|---|---|---|---|---|
| Porous Ag/$TiO_2$ | $3.3\times10^{-3}$ | $9.8\times10^{10}$ | 112/24 μs | $1.1\times10^{-6}$ | This work |
| Porous Au/Si | $3.5\times10^{-3}$ | – | – | – | [14] |
| Au nanorods/Si | $1\times10^{-5}$ | – | – | $2.5\times10^{-6}$ | [7] |
| Au/Pyramid-Si | $8.2\times10^{-3}$ | $1.8\times10^{10}$ | – | $1.5\times10^{-3}$ | [15] |
| Au/$SrTiO_3$/Si | $3.7\times10^{-4}$ | – | ~1 ms | $1.6\times10^{-2}$ | [20] |

Figure 2C, our device shows a fast response speed with $\tau_r$ of 112 μs and $\tau_f$ of 24 μs.

Moreover, the porous Ag/$TiO_2$ photodetector can also show a good photoresponse in the visible to near-infrared light region far away from the surface plasmon resonance wavelength. The responsivity values of the photodetector at 660 nm and 980 nm were 0.39 mA/W and 11 μA/W, respectively, and the detectivity values at 660 nm and 980 nm were $1.7\times10^{10}$ cmHz$^{1/2}$/W and $4.6\times10^{8}$ cmHz$^{1/2}$/W, respectively (Figure 3A and B). These results show that, although the responsivity of the detector decreases sharply with increasing light wavelength, a relatively high detectivity is still maintained owing to the low dark current. In addition, both in the visible light region and in the near-infrared region, the photocurrent of the device increases almost linearly with the light power, and the linear relationship keeps in a broad light power range (Figure 3C and D).

Table 1 summarizes the key metrics of our device and those of other reported photovoltaic plasmonic hot-electron photodetectors. In previous literature, most attention was focused on the responsivity (R) of the photodetectors, while other key metrics of the hot-electron photodetectors such as detectivity (D*) and response time ($\tau_r/\tau_f$) have remained largely unexplored. Our porous Ag/$TiO_2$ hot-electron photodetector shows a high responsivity that is comparable to the highest responsivity of photovoltaic hot-electron photodetectors [14, 15]. Furthermore, the response speed of our device is much faster than the previously reported values [20], and the detectivity and minimum detectable light intensity are also comparatively superior [15].

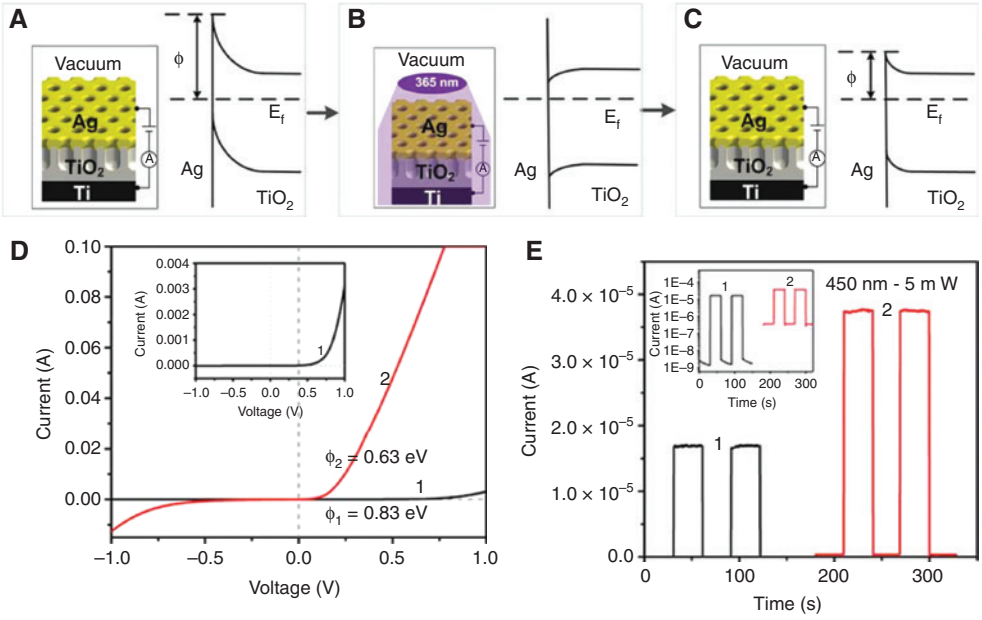


**Figure 4:** Responsivity improvement by decreasing Schottky barrier height.
(A–C) Schematic for the long-hours ultraviolet illumination treatment: the high Schottky barrier of the initial fabricated sample (A) can be eliminated by long-hours illumination under 365 nm light of 0.4 mW/cm² for 8 h (B), then a lower Schottky barrier will recover after turning off the 365 nm light. (D, E) I–V characteristics (D) and photocurrent response (E) of the porous Ag/$TiO_2$ heterojunction before (line 1) and after (line 2) long-hours ultraviolet illumination. The incident 450 nm light power in (E) is 5 mW, the inset is the same diagram with the Y-axis on the log 10 scale.

### 3.3 Improvement of the responsivity by decreasing Schottky barrier

Due to certain energy distribution of the hot-electrons [1], a lower Schottky barrier can enable more hot-electrons to cross over it and contribute to a higher responsivity. In our previous work, the Ag/$TiO_2$ Schottky barrier was proved to result from the chemisorbed oxygen on the surface of porous $TiO_2$, and the height of the Schottky barrier can be decreased by ultraviolet light illumination through a process of oxygen desorption, however, the decreased Schottky barrier will turn back to a high value as the ultraviolet light is turned off [24]. In order to obtain a permanent decreased Schottky barrier, we propose a method of long-hours ultraviolet light illumination in vacuum (Figure 4A–C). As shown in Figure 4A, the initial fabricated sample had a high Schottky barrier in vacuum due to the high doping of chemisorbed oxygen on the surface of $TiO_2$, and then a process of long-hours ultraviolet light illumination was carried out to remove the chemisorbed oxygen until the Schottky barrier was eliminated (Figure 4B). When the ultraviolet light is turned off, the Schottky barrier will recover gradually with re-chemisorption of the surrounding oxygen; but owing to the vacuum environment that cannot provide sufficient oxygen, only a lower Schottky barrier is eventually formed (Figure 4C).

After long-hours ultraviolet illumination, the I–V curves of the sample showed a weaker rectification characteristic (line 2 in Figure 4D) than the sample before ultraviolet illumination (line 1 in Figure 4D), and the barrier heights of the Ag/$TiO_2$ heterojunction before ($\phi_1$) and after ($\phi_2$) 365 nm light illumination were estimated to be 0.83 eV and 0.63 eV, respectively, based on the I–V curves (Figure S2 and Supplementary note), where line 1 is the same I–V curve as in Figure 1A. Figure 4E shows the photoresponse of the samples to the 450 nm light illumination with a power of 5 mW. As can be seen, the Ag/$TiO_2$ heterojunction after ultraviolet light illumination treatment showed a higher photocurrent (line 2 in Figure 4E), corresponding to a higher responsivity of 7.4 mA/W, however, the dark current also increased (line 2 in the inset of Figure 4E), which led to a lower detectivity of $1.2\times10^{10}$ cmHz$^{1/2}$/W. It can be concluded that while the low Schottky barrier is advantageous for obtaining high responsivity, it is simultaneously disadvantageous for detectivity.

## 4 Conclusions

In conclusion, we used thin porous $TiO_2$ to construct an Ag/$TiO_2$-Schottky-diode based hot-electron photodetector,

which had a broad response spectrum from visible to near-infrared. The responsivity, external quantum efficiency, detectivity, $I_l/I_d$ ratio, and response rise and fall time of the porous Ag/$TiO_2$ photodetector at 450 nm were calculated to be 3.3 mA/W, 0.91%, $9.8\times10^{10}$ cmHz$^{1/2}$/W, $1\times10^6$, 112 μs and 24 μs, respectively. The responsivity of our device was comparable to the highest responsivity value of the previously reported photovoltaic hot-electron photodetectors. At the same time, the high detectivity and fast response speed of the porous Ag/$TiO_2$ photodetector were much better than the previously reported hot-electron photodetectors. In addition, we further increased the responsivity of the photodetector from 3.4 mA/W to 7.4 mA/W by decreasing the barrier height of the Ag/$TiO_2$ Schottky junction.

This work provides inspiration for the performance improvement of the hot-electron photodetectors and material design of the metal/oxide-semiconductor based devices. With performance of microsecond-responses and high detectivity, the porous Ag/$TiO_2$ hot-electron photodetector will have a promising potential for a variety of imaging, optical communications and optical switches applications.

**Supplementary material:** X-ray diffraction pattern of the $TiO_2$/Ti, LnJ-V characteristics, calculation of the height of the Schottky barrier and transmission spectrum of the porous Ag/$TiO_2$ membrane.

**Acknowledgments:** This work was supported by the National Natural Science Foundation of China (Nos. 51701207, 51471162, 51502294, and 51671183), the CAS/SAFEA International Partnership Program for Creative Research Teams.

## References

[1] Sundararaman R, Narang P, Jermyn AS, Goddard WA, Atwater HA. Theoretical predictions for hot-carrier generation from surface plasmon decay. Nat Commun 2014;5:5788.
[2] Tan CF, Zing AKSS, Chen ZH, et al. Inverse stellation of CuAu-ZnO multimetallic-semiconductor nanostartube for plasmon-enhanced photocatalysis. ACS Nano 2018;12:4512–20.
[3] Zhang P, Wang T, Gong JL. Mechanistic understanding of the plasmonic enhancement for solar water splitting. Adv Mater 2015;27:5328–42.
[4] Gangadharan DT, Xu ZH, Liu YL, Izquierdo R, Ma DL. Recent advancements in plasmon-enhanced promising third-generation solar cells. Nanophotonics 2017;6:153–75.
[5] Liang FX, Ge CW, Zhang TF, et al. Plasmonic hollow gold nanoparticles induced high-performance $Bi_2S_3$ nanoribbon photodetector. Nanophotonics 2017;6:494–501.
[6] Li W, Valentine JG. Harvesting the loss: surface plasmon-based hot electron photodetection. Nanophotonics 2017;6:177–91.
[7] Knight MW, Sobhani H, Nordlander P, Halas NJ. Photodetection with active optical antennas. Science 2011;332:702–4.
[8] Berini P. Surface plasmon photodetectors and their applications. Laser Photonics Rev 2014;8:197–220.
[9] Othman N, Berini P. Nanoscale Schottky contact surface plasmon "point detectors" for optical beam scanning applications. Appl Opt 2017;56:3329–34.
[10] Alavirad M, Roy L, Berini P. Surface plasmon enhanced photodetectors based on internal photoemission. J Photon Energy 2016;6:042511.
[11] Huang JA, Luo LB. Low-dimensional plasmonic photodetectors: recent progress and future opportunities. Adv Opt Mater 2018;6:1701282.
[12] Xie BH, Fei GT, Xu SH, Gao XD, Zhang JX, Zhang DL. Tunable broadband wavelength-selective enhancement of responsivity in ordered Au-nanorod array-modified PbS photodetectors. J Mater Chem C 2018;6:1767–73.
[13] Sobhani A, Knight MW, Wang YM, et al. Narrowband photodetection in the near-infrared with a plasmon-induced hot electron device. Nat Commun 2013;4:1643.
[14] Lin KT, Chen HL, Lai YS, Yu CC. Silicon-based broadband antenna for high responsivity and polarization-insensitive photodetection at telecommunication wavelengths. Nat Commun 2014;5:3288.
[15] Qi ZY, Zhai YS, Wen L, et al. Au nanoparticle-decorated silicon pyramids for plasmon-enhanced hot electron near-infrared photodetection. Nanotechnology 2017;28:275202.
[16] Luo LB, Chen JJ, Wang MZ, et al. Near-infrared light photovoltaic detector based on GaAs nanocone array/monolayer graphene Schottky junction. Adv Funct Mater 2014;24:2794–800.
[17] Pescaglini A, Martin A, Cammi D, et al. Hot-electron injection in Au nanorod-ZnO nanowire hybrid device for near-infrared photodetection. Nano Lett 2014;14:6202–9.
[18] Wang WY, Klots A, Prasai D, Yang YM, Bolotin KI, Valentine J. Hot electron-based near-infrared photodetection using bilayer $MoS_2$. Nano Lett 2015;15:7440–4.
[19] Alavirad M, Olivieri A, Roy L, Berini P. High-responsivity sub-bandgap hot-hole plasmonic Schottky detectors. Opt Express 2016;24:22544–54.
[20] Matsui T, Li Y, Hsu MHM, et al. Highly stable plasmon induced hot hole transfer into silicon via a $SrTiO_3$ passivation interface. Adv Funct Mater 2018;28:1705829.
[21] Besteiro LV, Kong XT, Wang ZM, Hartland G, Govorov AO. Understanding hot-electron generation and plasmon relaxation in metal nanocrystals: quantum and classical mechanisms. ACS Photonics 2017;4:2759–81.
[22] Furube A, Du L, Hara K, Katoh R, Tachiya M. Ultrafast plasmon-induced electron transfer from gold nanodots into $TiO_2$ nanoparticles. J Am Chem Soc 2007;129:14852–3.
[23] Clavero C. Plasmon-induced hot-electron generation at nanoparticle/metal-oxide interfaces for photovoltaic and photocatalytic devices. Nat Photonics 2014;8:95–103.
[24] Gao XD, Fei GT, Zhang Y, Zhang LD, Hu ZM. All-optical-input transistors: light-controlled enhancement of plasmon-induced photocurrent. Adv Funct Mater 2018;28:1802288.
[25] Gao XD, Fei GT, Ouyang HM, et al. Ultrathin open-ended porous $TiO_2$ membranes for surface nanopatterning in fabricating nanodot arrays. Chem Commun 2014;50:14317–20.

[26] Xu JZ, Yang W, Chen HY, et al. Efficiency enhancement of $TiO_2$ self-powered UV photodetectors using a transparent Ag nanowire electrode. J Mater Chem C 2018;6:3334–40.
[27] Zheng LX, Hu K, Teng F, Fang XS. Novel UV-visible photodetector in photovoltaic mode with fast response and ultrahigh photosensitivity employing Se/$TiO_2$ nanotubes heterojunction. Small 2017;13:1602448.
[28] Genet C, Ebbesen TW. Light in tiny holes. Nature 2007;445:39–46.
[29] Moskovits M. Hot electrons cross boundaries. Science 2011;332:676–7.
[30] Zeng LH, Wang MZ, Hu H, et al. Monolayer graphene/germanium Schottky junction as high-performance self-driven infrared light photodetector. ACS Appl Mater Inter 2013;5:9362–6.
[31] An XH, Liu FZ, Jung YJ, Kar S. Tunable graphene-silicon heterojunctions for ultrasensitive photodetection. Nano Lett 2013;13:909–16.

**Supplementary Material:** The online version of this article offers supplementary material (https://doi.org/10.1515/nanoph-2019-0094).